

Anomalous magnetoresistance behavior of CoFe nano-oxide spin valves at low temperatures

J. Ventura,* J. B. Sousa, and M. A. Salgueiro da Silva

IFIMUP and Faculty of Sciences U. Porto, Rua do Campo Alegre, 678, 4169-007, Porto, Portugal

P. P. Freitas and A. Veloso

INESC, Solid State Technical Group, R. Alves Redol, 9-1, Lisbon, 1000, Portugal

We report magnetoresistance curves of CoFe nano-oxide specular spin valves of MnIr/CoFe/nano-oxidized CoFe/CoFe/Cu/CoFe/nano-oxidized CoFe/Ta at different temperatures from 300 to 20 K. We extend the Stoner-Wolfarth model of a common spin valve to a specular spin valve, introducing the separation of the pinned layer into two sublayers and their magnetic coupling across the nano-oxide. We study the effect of different coupling/exchange (between the antiferromagnetic layer and the bottom sublayer) field ratios on the magnetization and magnetoresistance, corresponding with the experimentally observed anomalous bumps in low temperature magnetoresistance curves.

I. INTRODUCTION

A simple spin valve¹ (SV) is a nanostructure with two ferromagnetic (FM) layers separated by a sufficiently thick nonmagnetic (NM) spacer. An adjacent antiferromagnetic (AFM) material fixes the magnetization of one of the FM layers, the so-called pinned layer. The other FM layer, called the free layer, is only weakly coupled (magnetically) to the pinned layer. Spin up and spin down electrons are differently scattered (either in the bulk or at the interfaces), usually producing a large magnetoresistance (MR) when a small applied magnetic field H reverses the free layer magnetization with respect to that of the pinned layer.

Recent reports on spin valves with the pinned and/or free layer partially oxidized,^{2,3,4} showed great MR enhancement over the conventional (nonoxidized) spin valves (CSV). Electrons are believed to reflect specularly at the nano-oxide layer (NOL)/FM interfaces, thus yielding higher MR ratios. Low temperature and temperature dependence studies of the transport and magnetic properties of NOL SVs can provide valuable information on the oxide layer properties, also assisting in the optimization of NOL SVs and corresponding physical understanding.^{3,5}

We previously reported⁵ the temperature dependence of the magnetoresistance $MR(H)$ curves for NOL SVs with the structure seed/MnIr/CoFe/oxidation (NOL1)/CoFe/Cu/CoFe/oxidation (NOL2). The first FM deposited layer (CoFe on MnIr) will be called the below-NOL1 pinned layer (FM_b) and its upper part is oxidized over an adequate thickness to form the NOL1 layer. The FM layer deposited after this oxidation will be called the above-NOL1 pinned layer (FM_a). The pinned layer thus consists of both FM_b and FM_a sublayers, sep-

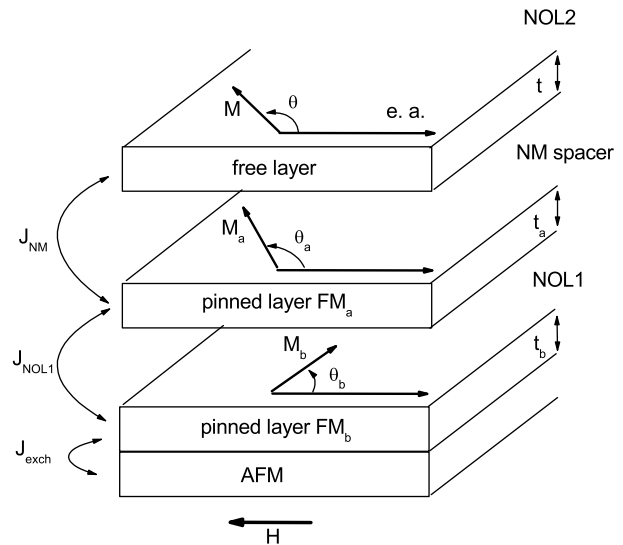


FIG. 1: Structure of a NOL SV.

arated by the NOL1 oxide layer. Our study⁵ included the temperature dependence of the $M(H)$ and $MR(H)$ curves for such NOL SVs, revealing the appearance of several anomalous features at low temperature, namely anomalous bumps in $MR(H)$ at intermediate fields and the absence of complete MR saturation up to large positive fields. In this article we focus on the physical origin of such features. For this we present a model based on the total energy⁶ of a NOL SV to describe the magnetization orientation in each of the three FM layers under an external magnetic field and the resulting $MR(H)$ behavior. We assume that the FM_b and FM_a layers are ferromagnetically coupled across NOL1 (Fig. 1),³ and study the effect of such coupling strength on the magnetization $M(H)$ and $MR(H)$ curves. The model accounts for the observed anomalous $MR(H)$ bumps,⁵ relating them to the M reversal in the pinned layer.

*Electronic address: joventur@fc.up.pt

The absence of full alignment in large positive fields at low temperature is discussed in terms of the permanence of 360° domain walls; the underlying H asymmetry is related to the dc field anneal. The key role played by the nano-oxide CoFe specular layers is also emphasized.

II. THEORETICAL MODEL

We extend the simple model describing the total energy of a CSV⁶ to the more complex structure of NOL SVs, explicitly introducing the pinned layer partition into the FM_b and FM_a sublayers separated by NOL1. The exchange coupling between the FM_b and AFM layers fixes the easy axis of the magnetization in the FM_b layer and (as a consequence of coupling interactions) in the FM_a and free layers. We assume coherent rotation of the magnetization within each layer, under an external magnetic field H. To simplify the treatment no anisotropy terms are included. The total energy per unit area E of a NOL SV is thus written as the sum of Zeeman E_{Zeeman} , coupling E_{coup} , and exchange E_{exch} energies (H along the easy axis):

$$E_{Zeeman} = -\mu_0 M_b t_b H \cos \theta_b - \mu_0 M_a t_a H \cos \theta_a - \mu_0 M t H \cos \theta, \quad (1)$$

$$E_{coup} = -J_{NOL1} \cos(\theta_b - \theta_a) - J_{NM} \cos(\theta_a - \theta), \quad (2)$$

$$E_{exch} = -J_{exch} \cos \theta_b. \quad (3)$$

M_b (θ_b), M_a (θ_a), and M (θ) are the saturation magnetizations (angles of the magnetization with the easy axis) in the FM_b, FM_a, and free layers, respectively. J_{NOL1} (J_{NM}) is the ferromagnetic exchange coupling energy per unit area between the FM_b and FM_a (FM_a and free FM) layers and J_{exch} is the exchange bias energy per unit area between the AFM and FM_b layers. Here t_b , t_a , and t are the thicknesses of the FM_b, FM_a (assumed equal), and free layers (thicker than the previous), respectively.

We numerically obtain the θ_b , θ_a , and θ angles which minimize E for each value of H and then calculate the total magnetic moment per unit area m of the NOL SV appearing along the easy axis:

$$m(H) = M_b t_b \cos(\theta_b(H)) + M_a t_a \cos(\theta_a(H)) + M t \cos(\theta(H)). \quad (4)$$

Dieny et al.⁷ showed that in a CoFe/Cu/SyAP/MnPt spin valve (SyAP: synthetic AFM⁸ pinned layer of CoFe/Ru/CoFe), the magnetoresistance associated with the two CoFe sublayers separated by Ru is only a small fraction of total MR. As a first approximation we then assume that MR is only due to the relative orientation of the magnetization in the FM_a and free layer:

$$MR(H) = \Delta R \left(\frac{1 - \cos[\theta_a(H) - \theta(H)]}{2} \right), \quad (5)$$

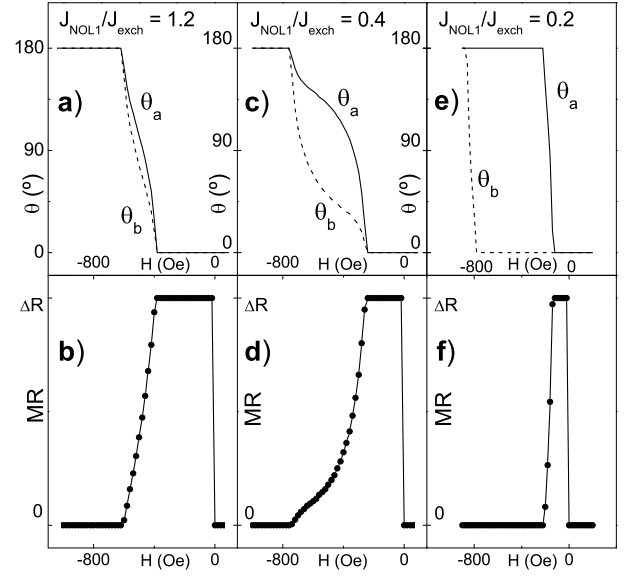


FIG. 2: Model simulations using different J_{exch} / J_{NOL1} ratios.

where ΔR is a characteristic amplitude. As expected for very small J_{NM} (across the spacer) the almost uncoupled free layer always reverses suddenly at very low negative values of H, but the model predicts three regimes for the rotation of the pinned layer at higher fields, depending on the J_{NOL1}/J_{exch} ratio:

(i) $J_{NOL1} > J_{exch}$ [Fig. 2(a)]: the magnetization of both FM_b and FM_a sublayers fully rotate ($0 \rightarrow \pi$) in a narrow field interval and always with approximately the same angle. This occurs because the large magnetic coupling between FM_b and FM_a (compared to J_{exch}) forces the two layers to behave as a (single) intra-pinned layer. Figure 2(b) shows the predicted MR(H) curve, displaying an abrupt MR drop when the magnetizations of FM_b and FM_a rotate.

(ii) $J_{NOL1} \leq J_{exch}$ [Fig. 2(c)]: both FM_b and FM_a layers reverse in the same field interval, but the corresponding range increases with decreasing J_{NOL1} and a considerable dephasing occurs between θ_b and θ_a at intermediate fields. Such increase in $(\theta_b - \theta_a)$ leads to broadening in the M(H) and MR(H) curves. Figure 2(d) illustrates, for $J_{NOL1} = 0.4 J_{exch}$, the predicted bump in the MR(H) curve at sufficiently negative fields.

(iii) $J_{NOL1} \ll J_{exch}$ [Fig. 2(e)]: the magnetizations of FM_b and FM_a now reverse almost individually and over distinct narrow field ranges; a small disturbance in the other's magnetization angle occurs in such ranges, producing also a disturbance in MR [Fig. 2(f)]. If J_{NOL1} is further decreased, both M_b and M_a reversals become truly independent, i.e., no change in the angle of the magnetization of one layer is visible when the other rotates. This produces three steps in the M(H) curve, corresponding to the magnetization reversal in the FM_b, FM_a, and free FM layers. No variation occurs in MR due to FM_b

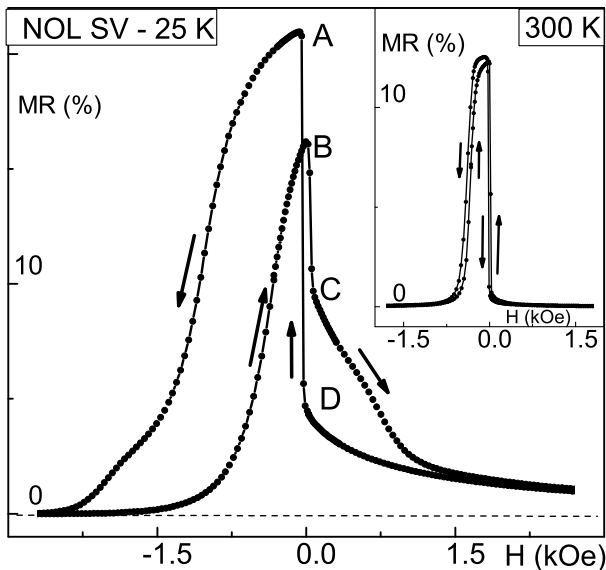


FIG. 3: Magnetoresistance of NOL SV at low (25 K) and high (300 K) temperature.

magnetization reversal [Eq. 5].

III. EXPERIMENTAL MR(T;H) BEHAVIOR

The details on the spin valves preparation and measurement techniques have been previously reported⁵ and will not be presented here. We simply comment that after being post-annealed in vacuum (10^{-6} Torr) at 270°C for 10 min the spin valves were cooled in a 3 kOe applied field, to impress an easy magnetic axis.

Room temperature MR(H) curves for a NOL SV with the structure Ta(67 Å)/Ni₈₁Fe₁₉(42 Å)/Mn₈₃Ir₁₇(90 Å)/CoFe(14 Å)/oxidation/Co₉₀Fe₁₀(15 Å)/Cu(22 Å)/Co₉₀Fe₁₀(40 Å)/oxidation/Ta(30 Å) exhibit the usual SV behavior (inset of Fig. 3): in a positive field both pinned and free layers are parallel aligned ($\uparrow\uparrow$), but the magnetization of the free layer abruptly reverses in a small negative field ($\downarrow\uparrow$ alignment results), leading to a high resistance over a finite ΔH range. Parallel alignment in the opposite sense ($\downarrow\downarrow$) ultimately occurs when the negative field overcomes the exchange bias between the AFM and the pinned layer, leading again to the low resistance state. The incorporation of the NOL greatly enhances the MR ratio over that observed in the corresponding nonspecular SV, from 5.9% to 12.5% at room temperature in our case. This ratio was found to increase linearly with decreasing temperature,⁵ due to the decrease in electron-spin wave scattering in the FM layers.⁹

With decreasing temperature the following features arise in the MR(H) curves of the NOL SV (Fig. 3):⁵ Large MR(H) broadening and the emergence of two anomalous MR bumps, one at each side; incomplete $\uparrow\uparrow$ alignment in

positive fields up to $H_{max} = 8$ kOe (MR does not vanish), whereas full $\downarrow\downarrow$ alignment (MR=0) occurs under moderate negative fields; absence of the usual ΔH plateau of constant (maximum) MR at low temperatures, indicating imperfect magnetization antiparallelism; and large hysteretic MR(H) cycles. These features are related to the presence of the NOL, since they are absent (or rather small) in the CSV.⁵

IV. DISCUSSION AND CONCLUSIONS

Increasing the applied field from negative H_{max} , where complete parallelism $\downarrow\downarrow$ occurs, initiates the M reversal of the pinned layer (exchange coupling with MnIr favors positive magnetization) producing a gradual MR increase. However, when the field reaches small positive values the free layer suddenly reverses its magnetization, producing a discontinuous MR decrease. One notices that the reversal of the pinned layer is still not complete since MR does not reach the value observed in the decreasing field regime (see Fig. 3 and below). To confirm that the rotation of the pinned layer continues under positive fields, we plot the difference between the maximum MR for decreasing and increasing fields (points A and B in Fig. 3) and the difference between after-free-layer-reversal in increasing and before-free-layer-reversal in decreasing fields (points C and D in the same figure) as a function of temperature (not shown). These differences are indeed similar, showing that the anomalous MR bump in positive fields is due to the incomplete reversal of the pinned layer. A rise of (both) these differences is visible below ~ 200 K, which may be related to the presence of an AFM oxide in the NOLs.

In MnIr/CoFe bilayers it was shown that magnetization reversal proceeds by coherent rotation, nucleation, and motion of domain walls.¹⁰ We believe that stable domain walls still remain in the pinned layer under positive fields and only gradually disappear as H increases, thus preventing full parallelism of the layer magnetic moments. In fact, at low temperature we were unable to achieve zero MR even at positive $H_{max} = 8$ kOe. It was recently found in CoFe thin films that 360° domain walls can indeed be stable up to high fields (rather than annihilating) and can give a significant contribution to the electrical resistance.¹¹

For decreasing fields from H_{max} , the free layer magnetization suddenly reverses at a small negative field but maximum MR (full magnetic antiparallelism FM_a/free layer) cannot be achieved due to the previous partial rotation/domain walls in the pinned layer; no ΔH plateau of maximum MR should then occur. Further field decrease keeps the ongoing rotation of the pinned layer and produces a broad decrease of the MR ratio due to the FM_b/FM_a coupling (see model in Sec. II). When the field value reaches the bump in the left side of the MR(H) curve, the rotation of the FM_a magnetization is almost complete, but FM_b is still far from complete rota-

tion [Figs. 2(c)-2(d)], due to the higher exchange pinning with the AFM. Complete parallel alignment is only obtained at a higher (negative) field. The model presented in Sec. II describes well important characteristics of this descending branch of the MR(H) curve (broadening and MR bump) for $J_{NOL1} \approx 0.4 J_{exch}$. Because these anomalous features appear and grow with decreasing temperature, one concludes that J_{NOL1} grows at a slower rate with decreasing temperature than J_{exch} .

The model we presented here gives a fair description of the anomalous bump present in the MR(H) curve at negative fields, correlating it to the presence of the FM_b layer in the NOL SV. However, the nonsaturation of MR at positive fields is not explained by our model and had to be explained in terms of irreversible processes (stable domain walls). The fact that this feature appears below

~ 200 K, the same temperature at which exchange and pinned layer coercive fields showed great enhancement¹² (thus suggesting the presence of an AFM phase) suggests that it is related to the magnetic order in the NOL1 layer. The magnetic structure of the MnIr layer can also have influence in the domain structure of the FM layer.¹³

Acknowledgments

Work supported by projects MMA/1787/95 and MMA/34155/99 from Fundação Ciência e Tecnologia, Portugal. J. O. Ventura is thankful for a FCT grant (SFRH/BD/7028/2001).

¹ B. Dieny, V. S. Speriosu, S. S. P. Parkin, B. A. Gurney, D. R. Wilhoit, and D. Mauri, *Phys. Rev. B* **43**, 1297 (1991).

² A. Veloso, P. P. Freitas, P. Wei, N. P. Barradas, J. C. Soares, B. Almeida, and J. B. Sousa, *Appl. Phys. Lett.* **77**, 1020 (2000).

³ M. F. Gillies and A. E. T. Kuiper, *J. Appl. Phys.* **88**, 5894 (2000).

⁴ H. Sakakima, M. Satomi, Y. Sugita, and Y. Kawawake, *J. Magn. Magn. Mater.* **210**, 20 (2000).

⁵ J. B. Sousa, J. O. Ventura, M. A. Salgueiro da Silva, P. P. Freitas, and A. Veloso, *J. Appl. Phys.* **91**, 5321 (2002).

⁶ M. R. Parker, H. Fujiwara, S. Hossain, and W. E. Webb, *IEEE Trans. Magn.* **31**, 2618 (1995).

⁷ B. Dieny, M. Li, S. H. Liao, C. Horng, and K. Ju, *J. Appl. Phys.* **87**, 3415 (2000).

⁸ A. Veloso and P. P. Freitas, *J. Appl. Phys.* **87**, 5744 (2000).

⁹ A. Chaiken, T. M. Tritt, D. J. Gillespie, J. J. Krebs, P. Lubitz, M. Z. Harford, and G. A. Prinz, *J. Appl. Phys.* **69**, 4798 (1991).

¹⁰ Y. G. Wang, A. K. Petford-Long, T. Hughes, H. Laidler, K. O'SGrady, and M. T. Kief, *J. Magn. Magn. Mater.* **242**, 1073 (2002).

¹¹ C. Tiusan, T. Dimopoulos, K. Ounadjela, M. Hehn, H. A. M. van den Berg, V. da Costa, and Y. Henry, *Phys. Rev. B* **61**, 580 (2000).

¹² J. O. Ventura, J. B. Sousa, M. A. Salgueiro da Silva, P. P. Freitas, and A. Veloso, *J. Magn. Magn. Mater.* **272**, 1892 (2004).

¹³ V. I. Nikitenko, V. S. Gornakov, A. J. Shapiro, R. D. Shull, K. Liu, S. M. Zhou, and C. L. Chien, *Phys. Rev. Lett.* **84**, 765 (2000).